

# Ras inhibits endoplasmic reticulum stress in human cancer cells with amplified *Myc*

Shira Yaari-Stark<sup>1</sup>, Maayan Shaked<sup>1</sup>, Yael Nevo-Caspi<sup>2</sup>, Jasmine Jacob-Hircsh<sup>3</sup>, Ron Shamir<sup>4</sup>, Gideon Rechavi<sup>2,3</sup> and Yoel Kloog<sup>1</sup>

<sup>1</sup> Department of Neurobiology, The George S. Wise Faculty of Life Sciences, Tel-Aviv University, Tel-Aviv, Israel

<sup>2</sup> Department of Pediatric Hematology-Oncology, Sheba Cancer Research Center, Sheba Medical Center, Tel-Hashomer, Tel-Aviv, Israel

<sup>3</sup> David and Inez Myers Laboratory for Genetic Research, Department of Human Genetics, Safra Children's Hospital, Sheba Medical Center, Tel Hashomer, and Sackler Faculty of Medicine, Tel-Aviv University, Tel-Aviv, Israel

<sup>4</sup> Blavatnik School of Computer Science, Tel-Aviv University, Tel-Aviv, Israel

In neuroblastoma LAN-1 cells harboring an amplified *MycN* gene, disruption of cooperation between Ras and MycN proteins by the Ras inhibitor farnesylthiosalicylic acid (FTS, Salirasib) reportedly arrests cell growth. Our aim was to establish whether this is a general phenomenon. We examined the effects of FTS on gene-expression profiles, growth and death of NCIH929 myeloma cells and K562 leukemia cells, which—like LAN-1 cells—exhibit *Myc* gene amplification and harbor active Ras. Under specified conditions, FTS reduced Ras and Myc and induced cell growth arrest and death in all *Myc*-amplified cell lines but not in SHEP, a neuroblastoma cell line without *Myc* gene amplification. Gene-expression analysis revealed a common pattern of FTS-induced endoplasmic reticulum (ER) stress, known as the unfolded protein response (UPR), in *Myc*-amplified cells, but not in SHEP. Thus, Ras negatively regulates ER stress in cells with amplified *Myc*. ER stress was also inducible by dominant-negative (DN)-Ras or shRNA to Ras isoforms, all of which induced an increase in BIP (the master regulator of ER stress) and its downstream targets Nrf2 and eIF2 $\alpha$ , both regulated by active p-PERK. FTS also induced an increase in p-PERK, while small interfering RNA to PERK reduced Nrf2 and ATF4 and rescued cells from FTS-induced death. BIP and its downstream targets were also increased by inhibitors of MAPK p38 and MEK. Ras, acting through MAPK p38 and MEK, negatively regulates the ER stress cascades BIP/PERK/Nrf2 and eIF2 $\alpha$ /ATF4/ATF3. These findings can explain the Ras-dependent protection of *Myc*-amplified cells from ER stress-associated death.

Ras proteins act as relay systems<sup>1</sup> where the active GTP-bound Ras activates a multitude of downstream effectors, including Raf-1, phosphoinositide 3-kinase (PI3K) and Ral-

GEFs, which regulate cell proliferation, differentiation, survival and death.<sup>2</sup> In many human tumors, Ras is chronically active.<sup>3</sup> This is largely attributable to activating mutations in *Ras* genes but also to alterations in upstream components, such as receptor tyrosine kinases that activate Ras.<sup>4,5</sup> Ras-GTP contributes to uncontrolled cell growth and cell death and—in cooperation with *Myc*, other oncogenes and tumor suppressors—leads to malignant transformation.<sup>6</sup>

A previous study demonstrated that in LAN-1 neuroblastoma cells, which harbor amplified *MycN*,<sup>7</sup> the Ras inhibitor farnesylthiosalicylic acid (FTS) induces growth arrest. This effect was accompanied by a marked decrease in MycN protein and reduced Ras signaling through the Raf/MEK/ERK and the PI3K/Akt cascades, resulting in a decrease in cyclin D1, retinoblastoma protein and E2F.<sup>7</sup> These findings suggested that Ras pathways regulate cell-cycle progression and mitosis in *MycN*-amplified neuroblastoma cells and showed that inhibition of Ras pathways can disrupt the cooperation between Ras and *Myc*.<sup>8</sup> It remained unknown, however, whether the phenomenon of “getting at *Myc* through Ras”<sup>9</sup> is a general phenomenon or is limited to *MycN* in neuroblastoma.

*Myc* gene amplification or mutational activation is a common occurrence in human cancers.<sup>8</sup> Gene amplification increases *Myc* gene copy number. For example, more than

**Key words:** stress, UPR, Nrf-2, HO-1, ATF, pEIF2 $\alpha$

**Abbreviations:** Ab: antibody; CML: chronic myeloid leukemia; DN: dominant-negative; eIF2 $\alpha$ : eukaryotic translation initiation factor 2 $\alpha$ ; ER: endoplasmic reticulum; ERK: extracellular signal-regulated kinase; FTS: farnesylthiosalicylic acid; GFP: green fluorescent protein; HO-1: heme oxygenase 1; JNK: c-JUN N-terminal kinase; PERK: PKR-like endoplasmic reticulum kinase; PI3K: phosphoinositide 3-kinase; RT: real-time; siRNA: small interfering RNAs; TF: transcription factor; TFBS: transcription factor binding site; UPR: unfolded protein response

Additional Supporting Information may be found in the online version of this article

**Grant sponsor:** The Israel Science Foundation; **Grant number:** 912/06; **Grant sponsor:** The Prajs-Drimmer Institute for the Development of Anti-Degenerative Drugs

**DOI:** 10.1002/ijc.25102

**History:** Received 12 Oct 2009; Accepted 24 Nov 2009; Online 8 Dec 2009

**Correspondence to:** Yoel Kloog, Department of Neurobiology, The George S. Wise Faculty of Life Sciences, Tel-Aviv University, 69978 Tel-Aviv, Israel, Tel: +092-3-640-9699, Fax: +972-3-640-7643, E-mail: kloog@post.tau.ac.il

200 copies per cell of N-Myc (*MycN*) can be found in neuroblastoma, and more than 50 copies per cell of *c-Myc*, *N-myc* or *L-myc* are found in small-cell lung cancers.<sup>10</sup> An increase in *c-Myc* gene transcription might account for the observed increase in Myc in human colon carcinoma.<sup>11</sup>

Here, we tested the hypothesis that disruption of the cooperation between Ras and Myc by inhibition of active Ras is a general phenomenon that can be exploited for the treatment of human cancers. To this end, we examined the effects of FTS on 3 different cell lines representative of distinct cancer types and distinct status of Myc and Ras. We used the previously studied LAN-1 cells,<sup>7</sup> which were shown to harbor amplified *MycN* and wild-type Ras.<sup>12</sup> We also used the NCIH929 myeloma cells that harbor amplified *c-Myc* and oncogenic N-Ras(13V)<sup>13</sup> and K562, the chronic myeloid leukemia (CML) blast crisis cells (K562) that harbor amplified *c-Myc* and contain the BCR-ABL fusion protein, which *inter alia* activates Ras.<sup>14</sup> It is important to note that the *ras* gene status in the cell lines under study is known. In neuroblastoma, *ras* gene mutation is relatively rare<sup>7,15</sup> and in CMLs as well.<sup>16</sup> Here, we used the cell lines described earlier because they represent the indicated combinations of Ras activation and *myc* amplification. It is not yet known which Ras isoform is the prominent active Ras in these cell lines. Here, we show that under specified conditions FTS reduced the total amounts of Ras and Myc proteins thereby inducing growth arrest and death in all cell lines.

## Material and Methods

### Cell lines and reagents

LAN-1, SHEP and NCIH929 cells were grown as detailed.<sup>7,17</sup> K562 cells were grown in RPMI. FTS was a gift from Concordia (Pharmaceuticals, Sunrise, FL). ECL kit was from Amersham (Arlington Heights, IL); Hoechst 33258 from Sigma-Aldrich (St. Louis, MO); SP600125 from Calbiochem (La Jolla, CA); LY294002, U0126 and SB203580 from AG Scientific (San Diego, CA). Antibodies used were as follows: mouse anti-pan-Ras antibodies (Ab-3) and mouse anti-MycN (Ab-1) (Calbiochem); mouse anti-*c-Myc* (C-33), rabbit anti-Nrf2 (H-300), rabbit anti-NQO1 (H-90), rabbit anti-ATF3 (C-19), rabbit anti-ATF4 (CREB2; C-20), goat anti-ATF6 $\alpha$  (C-18), mouse anti-GADD153 (B-3) and mouse anti-Bcl2 (C-2) (Santa Cruz Biotechnology, Santa Cruz, CA); mouse anti-phospho-ERK and rabbit anti-tubulin (AK-15) (Sigma-Aldrich); rabbit anti-heme-oxygenase-1 (HO-1) (SPA-895) (Stressgen Bioreagents, Victoria, BC, Canada); rabbit anti-phospho-Akt (ser473), rabbit anti-phospho-SAPK/JNK (Thr183/Tyr185), rabbit anti-phospho-p38 MAP kinase (Thr180/Tyr182), rabbit anti-GAPDH (14C10), rabbit anti-phospho-eIF2 $\alpha$  (ser51), rabbit anti-eIF2 $\alpha$  and rabbit anti-phospho-PKR-like endoplasmic reticulum kinase (anti-phospho-PERK; Thr980) (Cell Signaling Technology, Beverly, MA); rabbit anti-Bip/GRP78 (PA1-014A) (Affinity BioReagents, Suwanee, GA); rabbit anti-Bax NT and rabbit anti-Bak NT (Upstate, Lake Placid, NY) and peroxidase-goat anti-

rabbit IgG and peroxidase-goat anti-mouse IgG (Jackson ImmunoResearch Laboratories, West Grove, PA). Protein bands were quantified by densitometry with Image Master VDS-CL (Amersham Pharmacia Biotech, Piscataway, NJ).<sup>18</sup>

### Western blotting

LAN-1 ( $2 \times 10^6$  cells/10 cm) and K562 cells ( $0.2 \times 10^6$  cells/mL) were grown in RPMI 1640/5% FCS and NCIH929 cells ( $0.5 \times 10^6$  cells/mL) in ATTC medium/5% FCS. Cells were treated with 75  $\mu$ M FTS or with the vehicle (0.1% DMSO) for 24–72 hr, then lysed and subjected to SDS PAGE and immunoblot analysis as detailed earlier.<sup>18</sup>

### Cell growth under FTS treatment

LAN-1 and SHEP cells were grown in RPMI/5% FCS and treated with 50 or 75  $\mu$ M FTS or the vehicle (0.1% DMSO). Changes in cell morphology were recorded under a microscope. Hoechst staining was used for cell death estimation.<sup>7</sup> Phosphatidyl serine detection in the plasma membrane for the determination of cell death was performed by using the Annexin V-FITC assay kit according to the manufacturer's instructions (eBioscience). Cell populations were isolated by FACS sorting (FACSaria, Becton Dickinson). NCIH929 and K562 ( $2 \times 10^4$  cells/well in 96-well plates) were treated 3 hr after plating with 3–100  $\mu$ M FTS or the vehicle (0.1% DMSO). The apparent number of cells was estimated by means of the AlamarBlue assay according to the manufacturer's instructions (Serotec, Oxford, UK). Experiments were performed twice in quadruplicate.

### Cell proliferation assay

NCIH929 and K562 cells were plated in 5% FCS media at a density of  $2 \times 10^4$  cells/well in 96-well plates, and 3 hr later the cells were treated with 50, 75 or 100  $\mu$ M FTS or the vehicle (0.1% DMSO). Proliferation was assessed by incorporation of 5-bromo-2-deoxyuridine (BrdU), using the BrdU cell-proliferation assay kit (Calbiochem).

### Gene-expression profiling and analysis of expression data

All experiments were performed using Affymetrix Human Focus oligonucleotide arrays (Santa Clara, CA)—[http://www.affymetrix.com/support/technical/datasheets/human\\_datasheet.pdf](http://www.affymetrix.com/support/technical/datasheets/human_datasheet.pdf).

Total RNA was prepared as detailed previously—[http://bioinf.picr.man.ac.uk/mbcf/downloads/GeneChip\\_Target\\_Preparation\\_Protocol-CR-UK\\_v3.pdf](http://bioinf.picr.man.ac.uk/mbcf/downloads/GeneChip_Target_Preparation_Protocol-CR-UK_v3.pdf).<sup>7</sup>

FTS-treated cell samples were compared with samples of untreated cells, and differentially expressed genes were selected using *t*-test with a threshold *p*-value of 0.05 (Affymetrix MAS 5 algorithm). For the comparison of gene-expression profiles, we first filtered the probe sets of all 3 cell lines, representing 5 different conditions (drug treated *vs.* vehicle control, see Supporting Information Figs. 1a and 1b), retaining only probes detectable as “present” in at least 1 sample, and whose expression was flagged as “increased” or “decreased” under at least 1 FTS-treated condition (MAS 5

algorithm). The procedure generated a list of 4,230 probe sets. To identify common expression patterns induced in response to FTS treatment, we applied clustering analysis to the set of 1,218 genes whose expression was changed by at least 1.5-fold in at least 3 conditions (EXPANDER package<sup>19,20</sup>). Before clustering, the expression levels of each gene were standardized so that mean is equal to 0 and variance is equal to 1. For visualization purposes, we added to the data a dummy condition (column) representing “no change” level.<sup>17</sup> Additional analysis was applied to the 1,000 most active genes (ranked according to the magnitude of their log-ratios) as described in the Results section.

#### Real-time PCR for determination of *HO-1* and *NQO1* expression levels

Levels of expression of *HO-1* and *NQO1* were determined by real-time (RT) PCR using the iSCRIPT cDNA Kit (Bio-Rad, Hercules, CA) as described earlier<sup>7</sup> and in Supporting Information Table 1a. Expression of each gene was normalized using the expression levels of the housekeeping genes *HMBS* and *S14* as standards (<http://eng.sheba.co.il/genomics>).

#### Immunofluorescence for Nrf-2

LAN-1 ( $2 \times 10^5$ ) cells were plated on glass cover slips and treated with 5% FCS media and 75  $\mu$ M FTS or the vehicle (0.1% DMSO). The cells were fixed after 24 hr, permeabilized<sup>21</sup> and then labeled with Nrf2 antibody (Ab) by successive incubations with 2.5  $\mu$ g/mL anti-Nrf2 Ab and 5  $\mu$ g/mL Cy3-donkey anti-rabbit Ab (Jackson ImmunoResearch), as described.<sup>21</sup> For background staining, samples were stained in the absence of Nrf2 Ab. All other procedures were as detailed earlier.<sup>21,22</sup> Cells that were positive for nuclear-stained Nrf2 were counted.

#### Small interfering RNAs for PERK/EIF2AK2

Following an overnight incubation, LAN-1 cells were either not transfected (control) or transfected with 100 nM ON-TARGET<sup>plus</sup> siCONTROL nontargeting pool, 50 or 100 nM ON-TARGET<sup>plus</sup> PERK/EIF2AK2 small interfering RNA (siRNA) or transfection reagent alone (mock). As an indicator of transfected cells, we used the siGLO Green transfection indicator (Thermo Fisher Scientific (Dharmacon), Lafayette, CO). Transfection was performed with a Pierce kit according to the instructions in the manual (Rockford, IL). Transfected cells were incubated for 24 hr, then washed with ice-cold PBS and harvested with 100–200  $\mu$ L lysis buffer.<sup>18</sup> Cell lysates were subjected to SDS-PAGE followed by immunoblotting with mouse anti-EIF2AK2 Ab (Pierce, Rockford, IL). Alternatively, the transfectants were treated with 75  $\mu$ M FTS or DMSO and counted 24 hr later using the Hoechst dye-exclusion reagent. Images of total cells and fluorescent cells were then used to calculate the percentage of dead cells.

#### Establishment of shRNA knocked down in LAN-1 cells

The shRNA for *H-Ras*, *K-Ras* and *N-Ras* and a scrambled derivative (control) were purchased from Open Biosystems (Huntsville, AL) as described<sup>23</sup> and used for the establishment of LAN-1 cell stably expressing each of the shRNA. Selection medium containing 2  $\mu$ g/mL puromycin was used. Stable cells were harvested and analyzed by immunoblotting using anti-K-Ras, anti-H-Ras and anti-N-Ras Abs (1:50; Calbiochem).

#### Transfection of DN-Ras

LAN-1 cells ( $4 \times 10^6$  cells/sample) were electroporated with 2  $\mu$ g of dominant-negative (DN)-GFP-Ras (17N) or enhanced green fluorescent protein plasmid (pEGFP), using the Nucleofector device with the X-005 program and solution V (Amaxa Biosystems, Walkersville, MD). Cells were harvested 48 hr after transfection and analyzed by Western immunoblotting.

## Results

#### FTS downregulates Myc in cells with amplified Myc gene

Our aim was to determine, by comparing 3 different cell lines possessing chronically active Ras and amplified *Myc*, whether the disruption of Ras and *Myc* cooperation by the Ras inhibitor FTS is a general phenomenon. From earlier studies, we know that FTS treatment of glioblastoma alters the expression of hundreds of genes, causing both cell growth arrest and apoptosis.<sup>24</sup> We therefore decided to treat all of the *Myc*/Ras cell lines under conditions that would promote both cell growth arrest and cell death.<sup>24</sup>

The cells were grown in the presence of a relatively low serum concentration (5%) and were treated with FTS at 50 or 75  $\mu$ M. We found that the LAN-1 cells showed a marked reduction in growth and in addition underwent massive death (Fig. 1a, left upper panel). The effect of 75  $\mu$ M FTS was stronger than that of 50  $\mu$ M (Fig. 1a, left panel). Hoechst staining (Fig. 1a, right panel) and AnnexinV (Fig. 1b), both of which detect necrotic and apoptotic cells, confirmed the FTS-induced death of LAN-1 cells. By contrast, the SHEP cells, which bear only 1 copy of *MycN*, did not die but underwent growth arrest (Fig. 1a, lower panels). These results are important because they indicate that the FTS-induced death is associated with Ras/*MycN* cooperation. Treatment of LAN-1 cells grown in 5% serum with 75  $\mu$ M FTS indeed caused a reduction in Ras and *MycN* (Fig. 1c).

We next examined the effects of FTS under the above conditions on the growth and death of 2 other cell lines that exhibit amplified *c-Myc*, namely NCIH929 myeloma cells and K562 CML cells. FTS caused a dose-dependent decrease in the numbers of both NCIH929 and K562 cells (IC<sub>50</sub> 30–65  $\mu$ M; Fig. 2a). The decrease in cell number was due to inhibition of cell proliferation (evidenced by incorporation of the cell-proliferation marker BrdU; Fig. 2b, upper panel) and

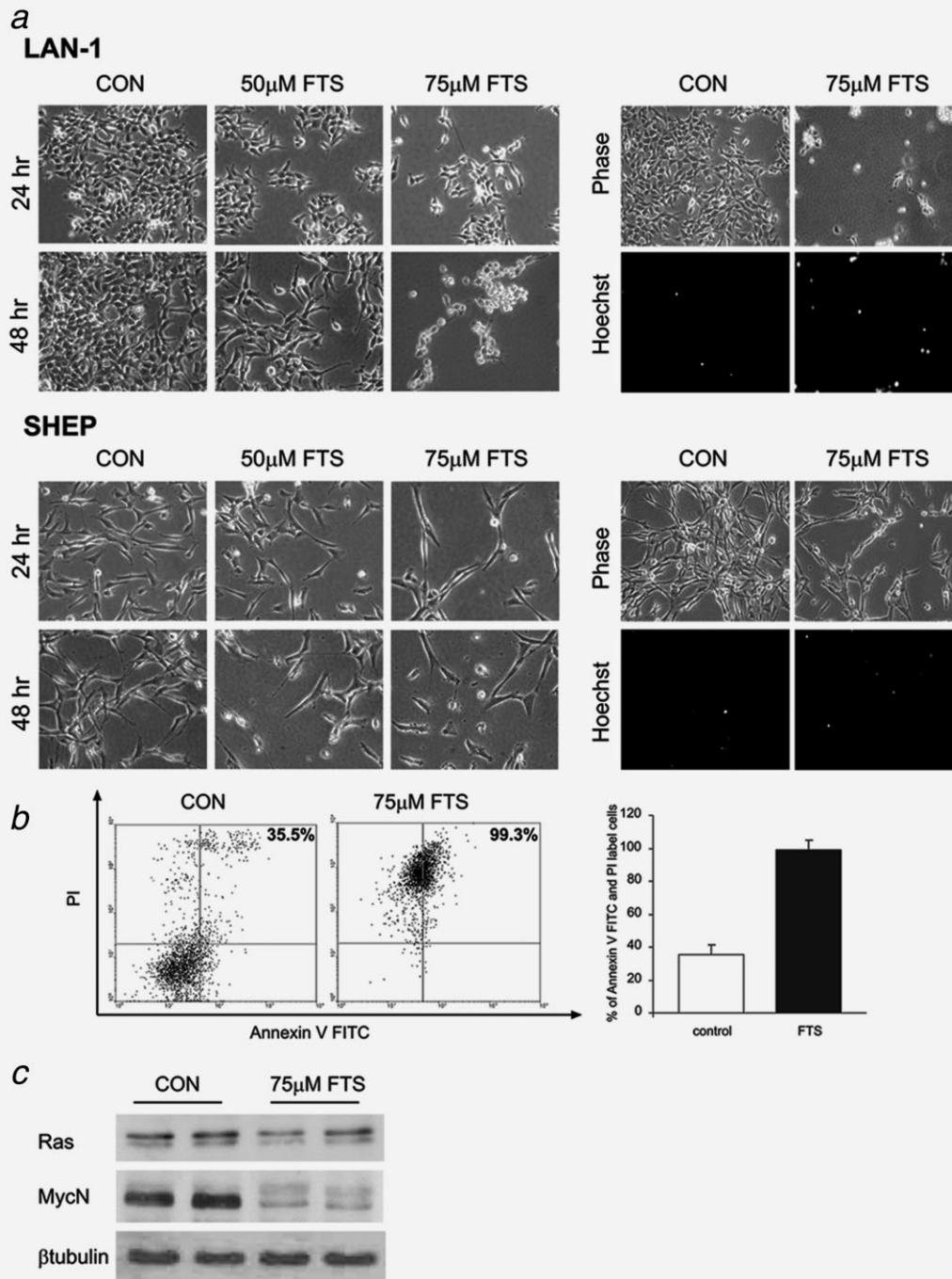


**Figure 1.** The Ras inhibitor farnesylthiosalicylic acid (FTS) induces growth arrest and death of LAN-1 neuroblastoma cells possessing an amplified *MycN* gene. (a) LAN-1 and SHEP neuroblastoma cells ( $2 \times 10^6$  cells/10-cm plate) were grown in the presence of a relatively low serum concentration (5%) and treated with 50 or 75  $\mu$ M FTS or 0.1% DMSO (control) for 24 or 48 hr (left panels). The figure shows Hoechst dye-exclusion staining of control and FTS-treated LAN-1 and SHEP cells. The cells were incubated for 48 hr in 5% media in the absence and presence of 75  $\mu$ M FTS, then stained with Hoechst 33258, as described in Material and Methods, and visualized under a fluorescence microscope ( $\times 20$ ). Typical phase and fluorescence images are shown (right panels). (b) Flow cytometry analysis of LAN-1 cells treated 48 hr with 75  $\mu$ M FTS. The Y-axis denotes the extent of propidium iodide (PI) labeling of cells nuclei, and the X-axis denotes the extent of AnnexinV-FITC labeling that binds to PS in the cell membrane (a measure of dead cells). The dot plot shows 4 populations: viable cells (lower left), apoptotic cells (lower right), apoptotic cells that have lost plasma membrane integrity (upper right) and necrotic cells (upper left). Note that the Annexin V-FITC assay detected a 64% increase in apoptotic and necrotic cells. (c) FTS downregulates Ras and MycN proteins in LAN-1 cells. LAN-1 cells were incubated for 24 hr in the absence and presence of 75  $\mu$ M FTS. The cells were then lysed, and aliquots of the cell lysate were subjected to SDS-PAGE and Western blotting with anti-Ras, anti-MycN and anti- $\beta$ -tubulin (loading control) Abs. Typical immunoblots of 1 of 3 experiments visualized by ECL are shown. FTS caused a reduction in Ras of  $25.1\% \pm 6.7\%$  and  $52\% \pm 8\%$  (mean  $\pm$  SD,  $n = 3$ ) in Ras and MycN, respectively.

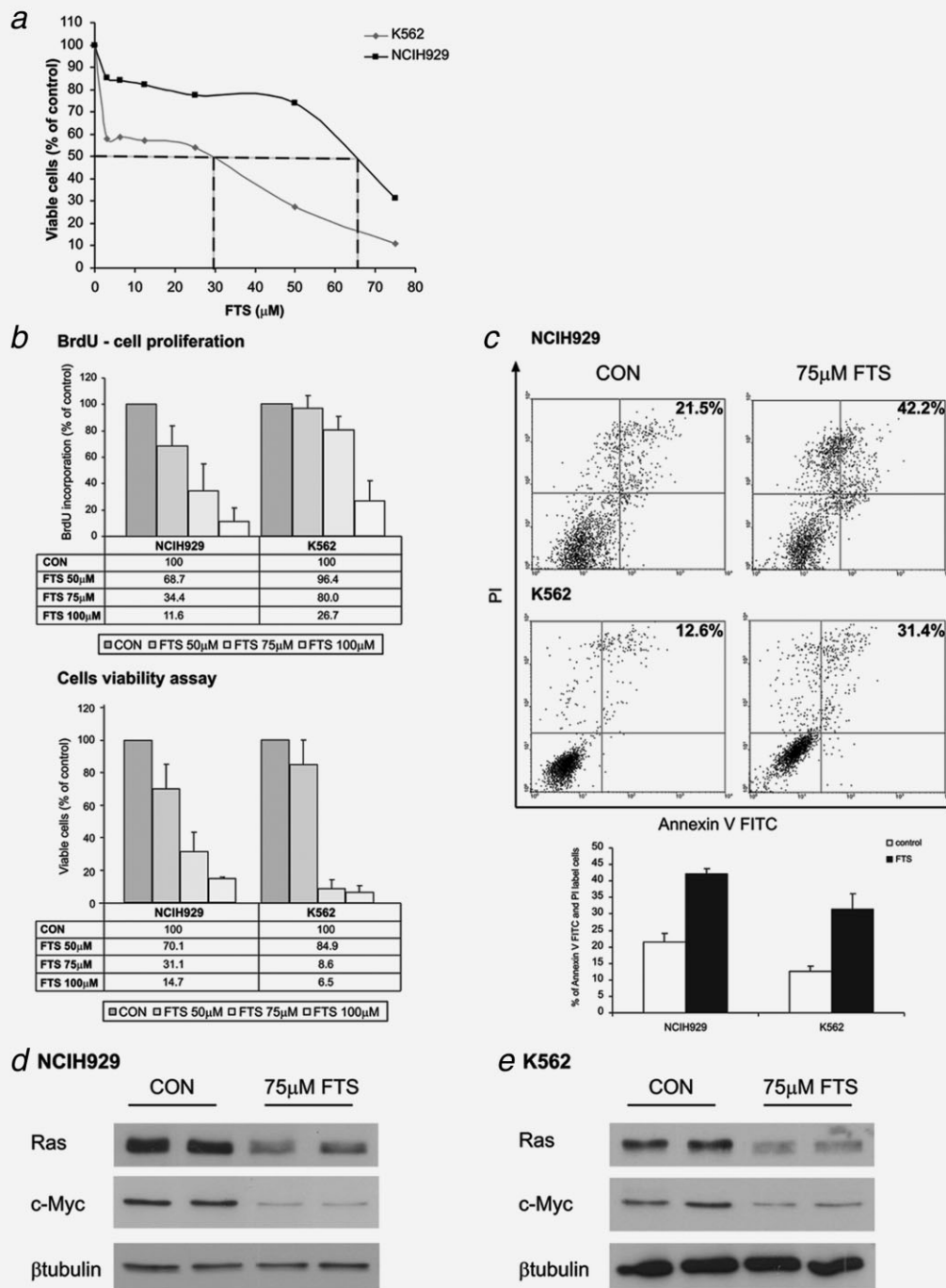


**Figure 2.** The Ras inhibitor farnesylthiosalicylic acid (FTS) inhibits the growth of NCIH929 myeloma and K562 CML cells possessing an amplified *c-Myc* gene. (a) NCIH929 and K562 cells ( $2 \times 10^4$  cells/well in 96-well plates) were incubated for 5 days in 5% FCS media in the absence and presence of the indicated concentrations of FTS. Cell viability was determined using AlamarBlue reagent. The Y-axis shows the numbers of cells in FTS-treated samples, calculated as a percentage of the total number of cells in the control (means  $\pm$  SD,  $n = 4$ ). (b) Reduction in cell proliferation by the indicated concentrations of FTS as determined by incorporation of BrdU into the DNA (means  $\pm$  SD,  $n = 3$ , left panel). Also shown is the growth inhibition of NCIH929 and K562 cells at the indicated concentrations determined by AlamarBlue values (right panel). (c) Flow cytometry analysis of NCIH929 and K562 cells treated 72 hr with 75  $\mu$ M FTS. The Y-axis denotes the extent of propidium iodide (PI) labeling of cells nuclei and the X-axis denotes the extent of Annexin-V-FITC labeling that binds to PS in the cell membrane (a measure of dead cells). The dot plot shows 4 populations: viable cells (lower left), apoptotic cells (lower right), apoptotic cells that have lost plasma membrane integrity (upper right) and necrotic cells (upper left). Note that the Annexin V-FITC assay detected a 20% increase in apoptotic and necrotic cells in both cell lines. (d, e) FTS downregulates Ras and Myc in cells with an amplified *Myc* gene. NCIH929 and K562 cells were incubated for 72 hr in the absence and presence of 75  $\mu$ M FTS. The cells were then lysed, and aliquots of the cell lysate were subjected to SDS-PAGE and Western blotting with anti-Ras, anti-c-Myc and anti- $\beta$ -tubulin (loading control) Abs. Typical immunoblots visualized by ECL are shown. Similar results were obtained in 2 additional experiments. FTS caused a significant reduction in Ras and in c-Myc in NCIH929 cells ( $41\% \pm 7\%$  and  $65\% \pm 3\%$ , respectively, mean  $\pm$  SD,  $n = 3$ ) and in the K562 cells ( $40\% \pm 10\%$  and  $57\% \pm 10\%$ , respectively, mean  $\pm$  SD,  $n = 3$ ).

induction of cell death (indicated by the cell viability reagent AlamarBlue; Fig. 2b, lower panel, and AnnexinV-FITC labeling, Fig. 2c). Thus, as in LAN-1 neuroblastoma cells, FTS (75  $\mu$ M) induced growth arrest and death of NCIH929 myeloma and K562 CML cells. Under these conditions, it also induced a marked decrease in Ras and c-Myc in both cell lines (Figs. 2d and 2e).

These results showed that FTS-induced reduction in the levels of Ras is accompanied by strong downregulation of Myc not only in neuroblastoma (7; Fig. 1c) but also in myeloma and leukemia (Figs. 2d and 2e). In these cell lines, all of which possess amplified *Myc* and chronically active Ras, FTS-induced inhibition of Ras inevitably disrupts the cooperation between Ras and Myc. Next, we examined whether the FTS treatment would induce significant changes in gene expression in all 3 cell lines under study.

#### Gene-expression profiling of FTS-treated cells harboring an amplified *Myc* gene

Gene-expression profiles of all 3 FTS-treated cell lines studied here showed marked alterations, which enabled us to perform a reliable comparative bioinformatics analysis of the effect of FTS under 5 different conditions (Supporting Information Figs. 1a and 1b, each condition refers to paired samples of the vehicle control and the drug-treated cells). For comparison of the sample profiles, we used a previously described hierarchical procedure,<sup>17</sup> which yielded a dendrogram with a primary partition according to cell line and a secondary partition reflecting FTS treatment (Supporting Information Fig. 1a). This indicated that our microarray measurements were robust, and moreover that they preserved the transcriptional behavior unique to each type of cell line, thus showing that the effect of tissue of origin on the expression profile is stronger than the effect resulting from the response to FTS.

To identify common expression patterns induced in response to FTS treatment, we subjected to cluster analysis the set of 1,218 genes whose expression was altered by at least a factor of 1.5 in at least 3 conditions (EXPANDER package,<sup>19,20</sup>). The CLICK clustering algorithm<sup>20</sup> identified 2 major clusters, representing decreased and increased steady-state mRNA levels: cluster 1 contained 290 genes whose expression was decreased by the FTS treatment, through all conditions sets, and cluster 2 contained 388 genes whose expression was increased by the FTS treatment in LAN-1 and K562 cell lines (Supporting Information Fig. 1c). Next, we sought transcriptional regulators that control these response patterns. To this aim, we applied EXPANDER's promoter-analysis algorithm PRIMA,<sup>25</sup> which searches for transcription factor binding site (TFBS) signatures whose prevalence is significantly high in promoters of the coclustered genes. PRIMA identified enrichment ( $p < 0.01$ ) of the transcription factors E2F-1 and NF-Y in cluster 1 and enrichment for the transcription factors Nrf-2, ATF4 and Bach2 in cluster 2. Increasing the stringency of our filtering, we applied cluster analysis to the set of 1,000 most reactive genes in our dataset, which

yielded an additional cluster, containing 151 genes whose expression was increased by FTS treatment, through all the condition sets. Importantly, as with the lower threshold analysis of the 1,218 genes here too, we detected enrichment in Nrf-2 (Supporting Information Fig. 1d).

Downregulation of E2F and NF-Y transcription factors by FTS is associated with inhibition of cell-cycle progression.<sup>26,27</sup> EXPANDER functional analysis of cluster 1 indeed showed enrichment of genes related to cell cycle, DNA replication, mitotic cell cycle, cell division, DNA metabolic process, nucleobase, nucleoside, nucleotide and nucleic acid metabolic process (Supporting Information Fig. 1e). Notably, genes related to nucleus and to nucleotide and nucleic acid metabolic functions are known to be transcriptionally controlled by Myc.<sup>28,29</sup>

The trend shown in clusters 2 and 3, affecting all 3 cell lines with amplified *Myc* gene, is significantly associated with the transcription factor Nrf2. Nrf2 regulates the activation of numerous genes in response to oxidative and/or electrophilic stress<sup>30</sup> and evidently also regulates genes for antioxidant enzymes, which provide the necessary protection against oxidative and electrophilic stress. Changes in expression of 28 Nrf2-regulated genes were detected in all 3 cancer cell lines under study (Supporting Information Table 2), including the prominent Nrf2-regulated genes *NQO1*, *NQO2* and heme oxygenase 1 (*HO-1*) (Supporting Information Table 3).

Another common pattern of genes whose expression was increased by FTS in the 3 cell lines was that of the transcription factors *ATF3*, *ATF4*, *ATF5* and *ATF6* (Supporting Information Table 3). ATFs, like Nrf2, are associated with stress responses.<sup>31</sup> More specifically, ATF4 and Nrf2 are known to act together in the unfolded protein response (UPR).<sup>31</sup> In addition, ATF3 attenuates the cell cycle under stress.<sup>32</sup> The predicted increase in the Nrf2 transcription factor in FTS-treated LAN-1 cells was confirmed by immunoblotting, which indicated a clear increase in Nrf2 protein in these cells ( $1.4 \pm 0.2$ -fold; mean  $\pm$  SD,  $n = 3$ , Fig. 3a) but not in SHEP (Fig. 3a). Similarly using RT-PCR, we confirmed the increase in *HO-1* and *NQO1* (Fig. 3b, upper panel). Notably, no such increase was observed in SHEP cells (Supporting Information Tables 1b and 1c), in which FTS did not induce cell death (Fig. 1a). Immunoblotting with anti-HO-1 and anti-NQO1 antibodies pointed to an increase in HO-1 and NQO1 proteins (by  $2.95 \pm 0.34$ -fold and  $1.7 \pm 0.4$ -fold, respectively; means  $\pm$  SD,  $n = 3$ ; Fig. 3b, lower panel). Finally and consistently with the gene-profiling analysis, we also found an increase in HO-1 and ATF3 in FTS-treated LAN-1, NCIH929 and K562 cells (Fig. 3c). Increase in the levels of GADD153, Bak and Bax and decrease in Bcl2 protein were observed as well (Fig. 3c). Importantly, elevated GADD153 expression is known to downregulate Bcl2 expression in ER stress.<sup>33</sup> Also, the proapoptotic Bax and Bak proteins are known to modulate the UPR by a direct interaction with IRE1 $\alpha$  (<sup>34</sup>; the UPR; Fig. 4a).

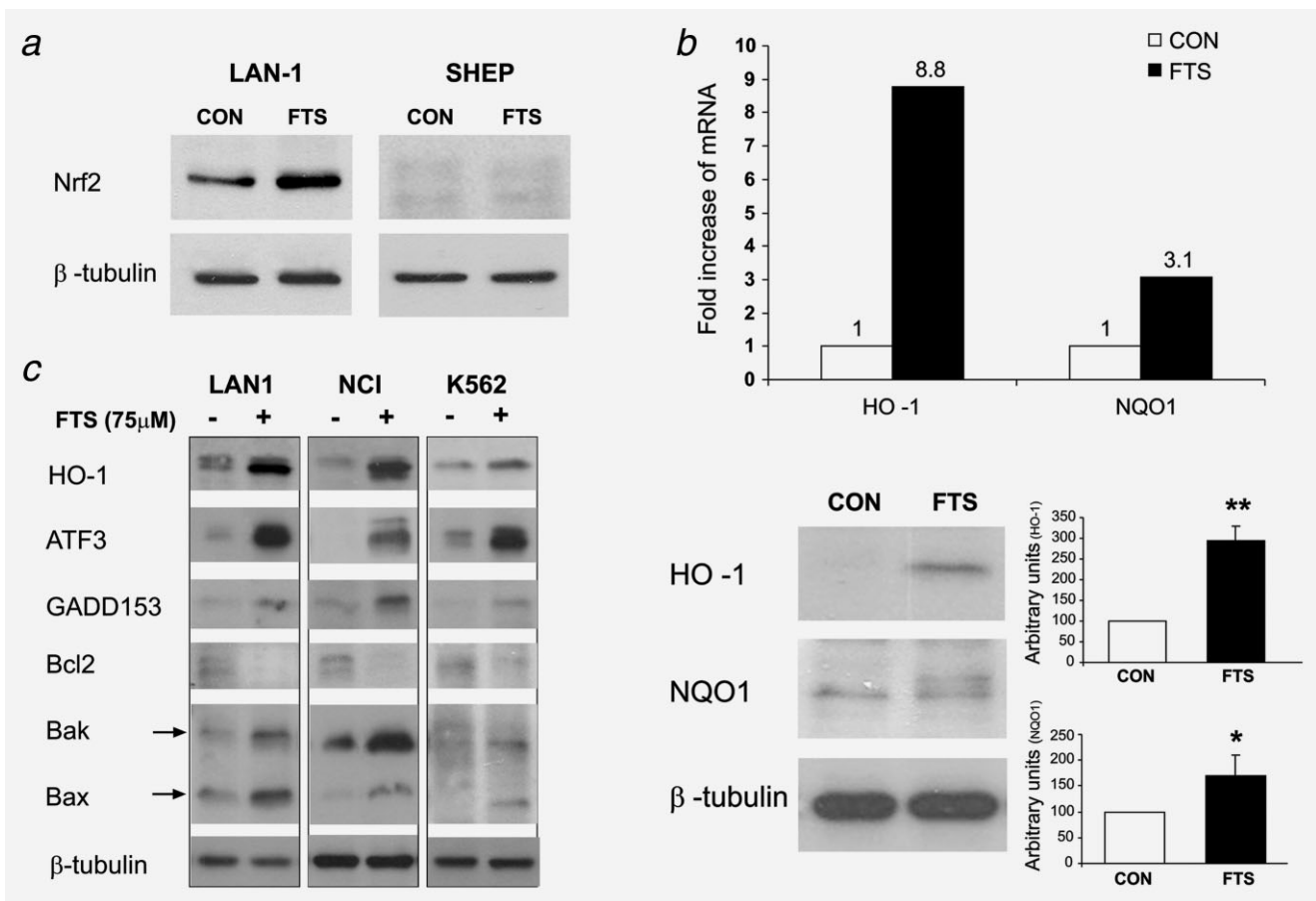


**Figure 3.** Farnesylthiosalicylic acid (FTS) upregulates the transcription factors Nrf2 and induces an increase in the amounts of *HO-1* and *NQO1* mRNA and protein in LAN-1 cells. LAN-1 (*a–c*) and SHEP (*a*) neuroblastoma cells were cultured and treated with 75  $\mu$ M FTS or 0.1% DMSO (control) for 24 hr, as described in Figure 1. The cells were then lysed. (*a*) Quantitative determination of Nrf2 in LAN-1 (left) and SHEP (right) cells by Western blotting. Composite densitometry of 3 experiments in LAN-1 cells showed a  $44.5\% \pm 2\%$  increase in Nrf2 protein after FTS treatment when compared with controls ( $p < 0.001$ , Student's *t*-test). No differences were observed in the SHEP cells lysates. (*b*) Cells were harvested and prepared for reverse transcriptase analysis, as described previously.<sup>7</sup> Samples were quantitatively analyzed for *HO-1* and *NQO1* mRNA relative to *HMBS*, the housekeeping gene (upper panel). Shown are *HO-1* and *NQO1*, determined by Western blotting analysis (lower panel). Composite densitometry of 3 experiments is shown on the right. \* $p < 0.05$ , \*\* $p < 0.001$ , Student's *t*-test. (*c*) Cancer cells were grown in 5% FCS media, in the absence or presence of 75  $\mu$ M FTS, for 24 hr (LAN-1) or 72 hr (NCIH929 and K562). Cells were lysed and *HO-1*, *ATF3*, *GADD153*, *Bcl2*, *Bax* and *Bak* were quantitatively determined by immunoblot analysis using specific antibodies.  $\beta$ -Tubulin is included as a control for equal protein loading. Similar results were obtained in 2 additional experiments.

Taken together, these results showed for the first time that FTS can induce a stress response (the UPR; Fig. 4*a*) in cells with amplified *Myc*. In other words, chronically active Ras, in cooperation with *Myc*, inhibits stress responses.

#### Reduction in the levels of Ras triggers the unfolded protein response cascade in LAN-1 cells

Next we examined the effects of FTS on BIP (GRP78), an ER-resident chaperon known as a master regulator of the ER and is upregulated during the stress response (the UPR; Fig. 4*a*).<sup>31</sup> BIP was rapidly increased in FTS-treated LAN-1 cells

(within 3–24 hr, Fig. 4*b*). Transcription of BIP is under the control of ATF6 (<sup>31</sup>; Fig. 4*a*), and we found that FTS indeed induced a time-dependent increase in ATF6 (Fig. 4*b*).

BIP regulates the activity of PERK/EIF2AK3 (<sup>31</sup>; Fig. 4*a*). PERK in turn activates Nrf2, inducing its release from the protein Keap1. This results in Nrf2 cytoplasmic-to-nuclear translocation and increased transcription of Nrf2 target genes.<sup>31</sup> Consistently with the hypothesis that inhibition of active Ras by FTS induces the UPR, including PERK activation, we found that FTS treatment in LAN-1 cells induced a robust translocation of Nrf2 from the cytoplasm to the nucleus (Fig. 4*c*).

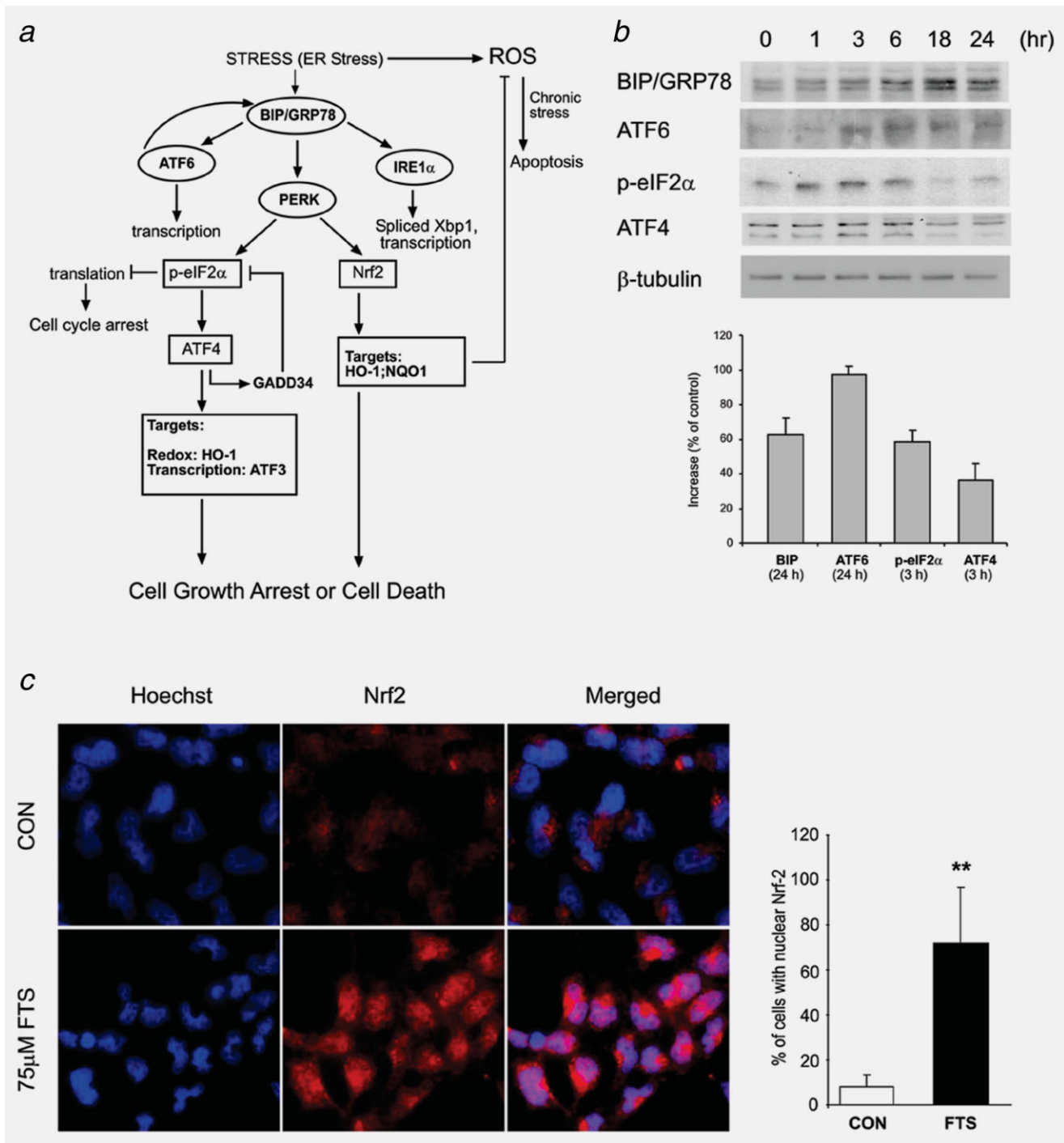
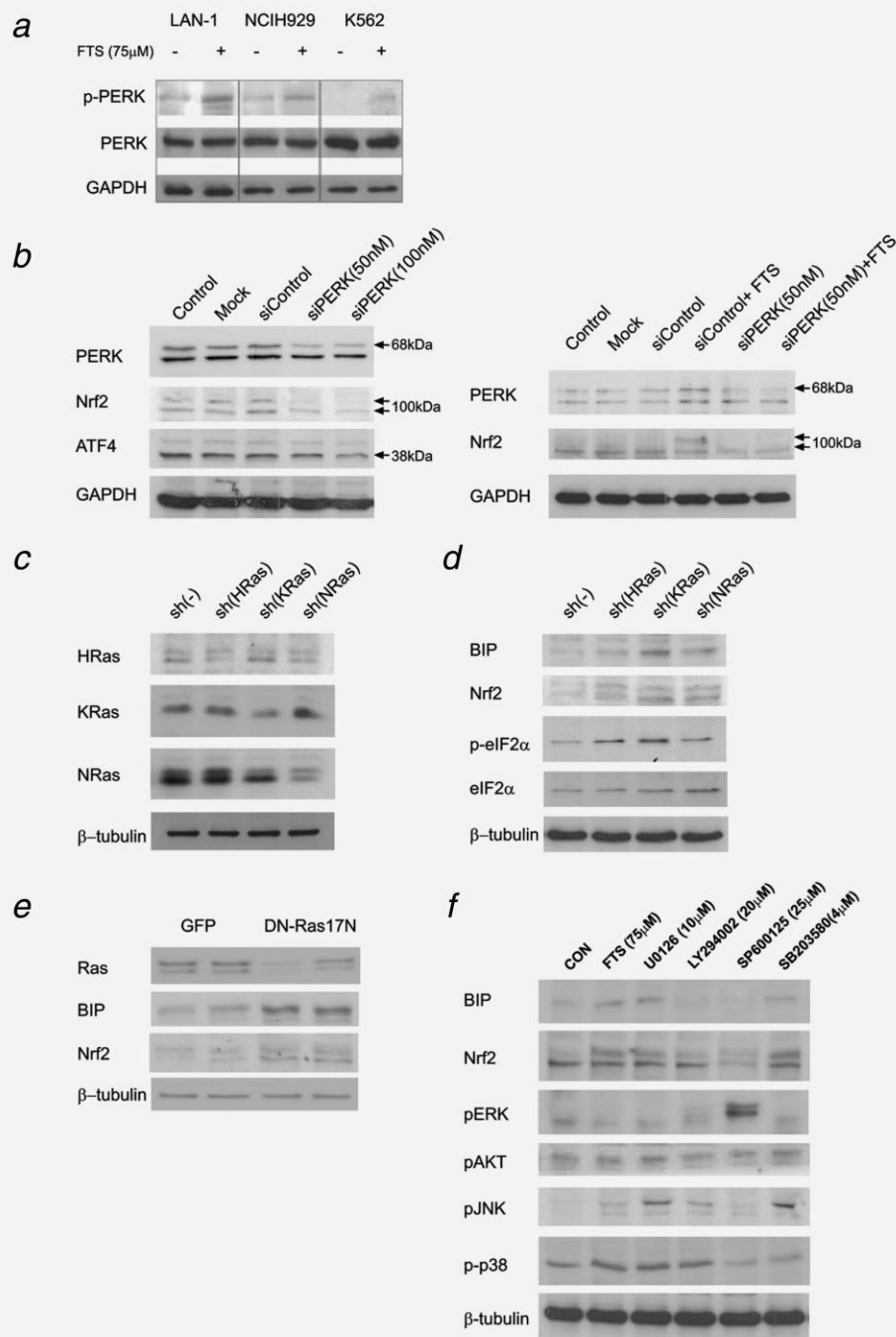


Figure 4. A decreased Ras levels trigger the unfolded protein response (UPR) cascade in LAN-1. (a) Schematic presentation of the UPR cascade according to Ref. 31. ROS: reactive oxygen species. (b) LAN-1 cells were treated for 0, 1, 3, 6, 18 or 24 hr with 75  $\mu$ M farnesylthiosalicylic acid (FTS) in 5% FCS media. Cells were then lysed and samples subjected to SDS-PAGE and examined by immunoblotting with specific antibodies. The recorded increase in the examined proteins relatively to the control was as follows. BIP/GRP78 62%  $\pm$  9.8%, ATF6 97%  $\pm$  4.2%, p-eIF2 $\alpha$  58%  $\pm$  6.2% and ATF4 36%  $\pm$  9.4% were examined by immunoblotting with specific antibodies. Composite densitometry of each protein (mean  $\pm$  SD,  $n$  = 3) is shown (lower panel). (c) Nuclear localization of Nrf2 following treatment of LAN-1 cells with FTS for 24 hr. Typical fluorescence images (red, Nrf2; blue, Hoechst-stained nuclei) are shown. Statistical analysis of the results is shown in the right panel. Data are expressed in terms of numbers of cells with nuclear Nrf2 in FTS-treated samples relative to control samples ( $n$  = 10, \*\* $p$  < 0.001, Student's  $t$ -test).



**Figure 5.** A decreased Ras levels triggers the unfolded protein response cascade. (a) The UPR is dependent on PKR-like endoplasmic reticulum kinase (PERK). Farnesylthiosalicylic acid (FTS) induces an increase in p-PERK. Cancer cells were grown in 5% FCS media, in the absence or presence of 75  $\mu$ M FTS, for 24 hr (LAN-1) or 72 hr (NCIH929 and K562). Cells were then lysed and p-PERK (Thr980) and PERK were quantitatively determined by immunoblotting with specific antibodies. (b) Induction of Nrf2 and ATF4 in LAN-1 cells is PERK dependent. LAN-1 cells were transfected and then lysed 24 hr later, alternatively, medium was replaced by 5% FCS media 1 day later, and the cells were incubated with 75  $\mu$ M FTS or vehicle control for an additional 24 hr. Control cells were not transfected. Cells were transfected with transfection reagent alone (mock), with 100 nM ON-TARGETplus *siCONTROL* nontargeting pool, with 50 nM ON-TARGETplus SMARTpool *siRNA* (*siPERK*) or with 100 nM ON-TARGETplus SMARTpool *siRNA* (*siPERK*). Western blot data for GAPDH are included as a control for equal protein loading. Decrease in Nrf2 and ATF4 was 43%  $\pm$  5% and 39%  $\pm$  0.7%, respectively. (c–f) The unfolded protein response (UPR) is negatively regulated by Ras in LAN-1 cells. shRNA for *H-Ras*, *K-Ras* and *N-Ras* and a scrambled derivative (sh(–)) were retrovirally introduced into LAN-1 cells, and the expression of (c) each Ras isoform and of (d) BIP, Nrf2, p-eIF2 $\alpha$  (ser51) and eIF2 $\alpha$  were then determined by Western blotting, as described in Material and Methods. The mean decrease in Ras isoforms expression (mean  $\pm$  SD,  $n = 3$ ) was 22%  $\pm$  5%, 35%  $\pm$  3.7% and 43%  $\pm$  2% in H-, K- and N-Ras, respectively. (e) LAN-1 cells were transfected with DN-Ras-GFP or GFP plasmid (GFP), and BIP and Nrf2 were then quantitatively determined by Western blotting with specific antibodies, as described in Material and Methods. Duplicate samples are shown. (f) LAN-1 cells were plated ( $2 \times 10^6$  cells/10-cm plate). The medium was replaced 1 day later with 5% FCS media, and cells were treated with 0.1% DMSO (control) or farnesylthiosalicylic acid (FTS) (75  $\mu$ M), U0126 (10  $\mu$ M), LY294002 (20  $\mu$ M), SP600125 (25  $\mu$ M) or SB203580 (4  $\mu$ M). Cells were lysed 24 hr after treatment. Samples were subjected to SDS-PAGE, and BIP, Nrf2, pERK, pAkt, pJNK and p-p38 were each quantitatively determined by Western analysis.  $\beta$ -Tubulin is included as a control for equal protein loading. Typical immunoblots for all experiments are shown. Similar results were obtained in 3 additional experiments.

PERK also phosphorylates and activates the eukaryotic translation initiation factor 2 $\alpha$  (eIF2 $\alpha$ ), a central mediator in attenuation of protein translation, resulting in a decrease in the amount of client proteins traversing the ER (<sup>31</sup>; Fig. 4a). We therefore next examined the effects of FTS on activation of eIF2 $\alpha$  and found a transient increase in p-eIF2 $\alpha$  within 3–6 hr of FTS treatment (Fig. 4b). Active eIF2 $\alpha$  is known to enhance translation of ATF4. Consistently with the transient increase in p-eIF2 $\alpha$ , we also found a transient increase in ATF4 (Fig. 4b). In line with the FTS-induced increase in BIP (Fig. 4b), we found that FTS induced an increase in p-PERK in all 3 cell lines studied (Fig. 5a).

Taken together, these results strongly suggest that FTS triggers the BIP/PERK/eIF2 $\alpha$  and Nrf2 (Figs. 3, 4 and 5a) signaling cascades that regulate the typical UPR and its specific effects on transcription.

To confirm the dependence of Nrf2 and ATF4 on PERK in LAN-1 cells, we used the siRNA approach, in which LAN-1 cells are transfected with *PERK* siRNA SMARTpool (*siPERK*). PERK was reduced in these transfected cells (46%  $\pm$  6.5% reduction) relative to nontransfected control cells or to the transfection reagent alone (mock) or to *siCONTROL* (nontargeting pool) (Fig. 5b). Concomitantly, both Nrf2 and ATF4 were decreased (Fig. 5b, left panel), confirming that their expression depends on PERK. In addition, we found that *siPERK* blocked the FTS-induced increase in the levels of Nrf2 protein (Fig. 5b, right panel).

### The UPR is negatively regulated by Ras in LAN-1 cells

The results described earlier implied that Ras negatively regulates the UPR in cells bearing an amplified *Myc* gene. To examine this possibility directly, we used shRNAs for each of the Ras isoforms (*H-Ras*, *K-Ras* and *N-Ras*) as described<sup>23</sup> and established stable LAN-1 cell lines, each with one of the Ras isoform shRNAs. We then examined the quantitative effects of Ras downregulation on BIP, Nrf2 and p-eIF2 $\alpha$  as readouts. As a control, we used a cell line infected with an empty vector. Each of the established cell lines exhibited a significant reduction in the corresponding Ras isoform (Fig. 5c).

Next we determined the amounts of BIP, Nrf2 and active p-eIF2 $\alpha$  in each of the cell lines. We found a significant increase in BIP and in Nrf2 compared with the control. The effect was more pronounced in the shK-Ras and shN-Ras (fold increases respectively were 1.4  $\pm$  0.1 and 1.2  $\pm$  0.03 in BIP and 1.4  $\pm$  0.06 and 1.35  $\pm$  0.09 in Nrf2). We also found that p-eIF2 $\alpha$  was increased relative to the control (fold increases in the shH-Ras, shK-Ras and shN-Ras cells were 3.6  $\pm$  0.04, 4.0  $\pm$  0.015 and 2.4  $\pm$  0.05, respectively; Fig. 5d). These results indicate that each of the Ras isoforms can negatively regulate the UPR. Interestingly, although individual downregulation of each Ras isoform caused a 2- to 4-fold increase in p-eIF2 $\alpha$ , the effect of FTS, which acts on all Ras isoforms,<sup>35</sup> was much stronger (fold increase of 5.8  $\pm$  0.06; Fig. 4b), reflecting the inhibitory action of FTS on all Ras isoforms.<sup>35</sup> DN-

Ras, like FTS, indeed caused a significant increase in BIP and Nrf2 (Fig. 5e) or in p-eIF2 $\alpha$  (not shown).

Next we examined how which of the known Ras signaling pathways is involved in the upregulation of Nrf2. We focused on ERK, c-JUN N-terminal kinase (JNK) and p38 signaling pathways because they each play a role in Nrf2 upregulation<sup>36</sup> and because the JNK/c-JUN pathway is associated with survival and the stress response.<sup>37,38</sup> LAN-1 cells were incubated with 75  $\mu$ M FTS or with 10  $\mu$ M U0126 (MEK inhibitor), 20  $\mu$ M LY294002 (PI3K inhibitor), 25  $\mu$ M SP600125 (JNK inhibitor), 4  $\mu$ M SB203580 (p38 inhibitor) or with the vehicle (control) for 24 hr. Cell lysates were then subjected to immunoblot analysis with anti-BIP, anti-Nrf2, anti-pERK, anti-pAKT, anti-pJNK and anti-p-p38 Abs. Separate immunoblots of pERK, pAKT, pJNK and p-p38 confirmed the inhibitory activity of each of the inhibitors (Fig. 5f). MEK and p38 inhibitors induced significant increases in BIP and Nrf2 proteins, resembling those induced by FTS (Fig. 5f). No significant changes in the amounts of BIP or Nrf2 protein were found after treatment with LY294002 (a PI3K inhibitor). The JNK inhibitor SP600125, however, caused a significant decrease in both BIP and Nrf2. Taken together, these results suggest that the Ras pathways Raf/MEK/ERK and MKK3/6/p38 negatively regulate BIP and Nrf2 in LAN-1 cells, whereas the SAPK/JNK pathway positively regulates them.

### Downregulation of PERK rescues LAN-1 cells from FTS-induced death

We next investigated whether the 2 responses, ER stress and cell death, which are apparent in LAN-1 but not in SHEP cells treated with the Ras inhibitor FTS, are related. To this end, we examined whether downregulation of PERK can rescue LAN-1 cells from death induced by FTS. LAN-1 cells were transfected with either *PERK* siRNA SMARTpool (*siPERK*) or *siCONTROL* (nontargeting pool), as described earlier, and then treated with 75  $\mu$ M FTS or with vehicle for an additional 24 hr. The results of these experiments are presented in Figure 6a. As shown, LAN-1 cells that were transfected with *siCONTROL* (nontargeting pool) sustained massive death when treated with 75  $\mu$ M FTS (Figs. 6a and 6b). In marked contrast, the death rate of LAN-1 cells that were transfected with *siPERK* and treated with 75  $\mu$ M FTS was low (Figs. 6a and 6b). These results established that the FTS-induced death of LAN-1 cells depends on PERK, *i.e.*, on the ER stress. Note that the transfection by itself had no effect on the ability of FTS to inhibit LAN-1 cell growth, as determined by direct counting of live cells (Fig. 6c). These assays showed, however, that growth inhibition by FTS was attenuated by *siPERK* (Fig. 6c), in line with previous reports that activation of the stress response results in cell growth arrest.<sup>31</sup>

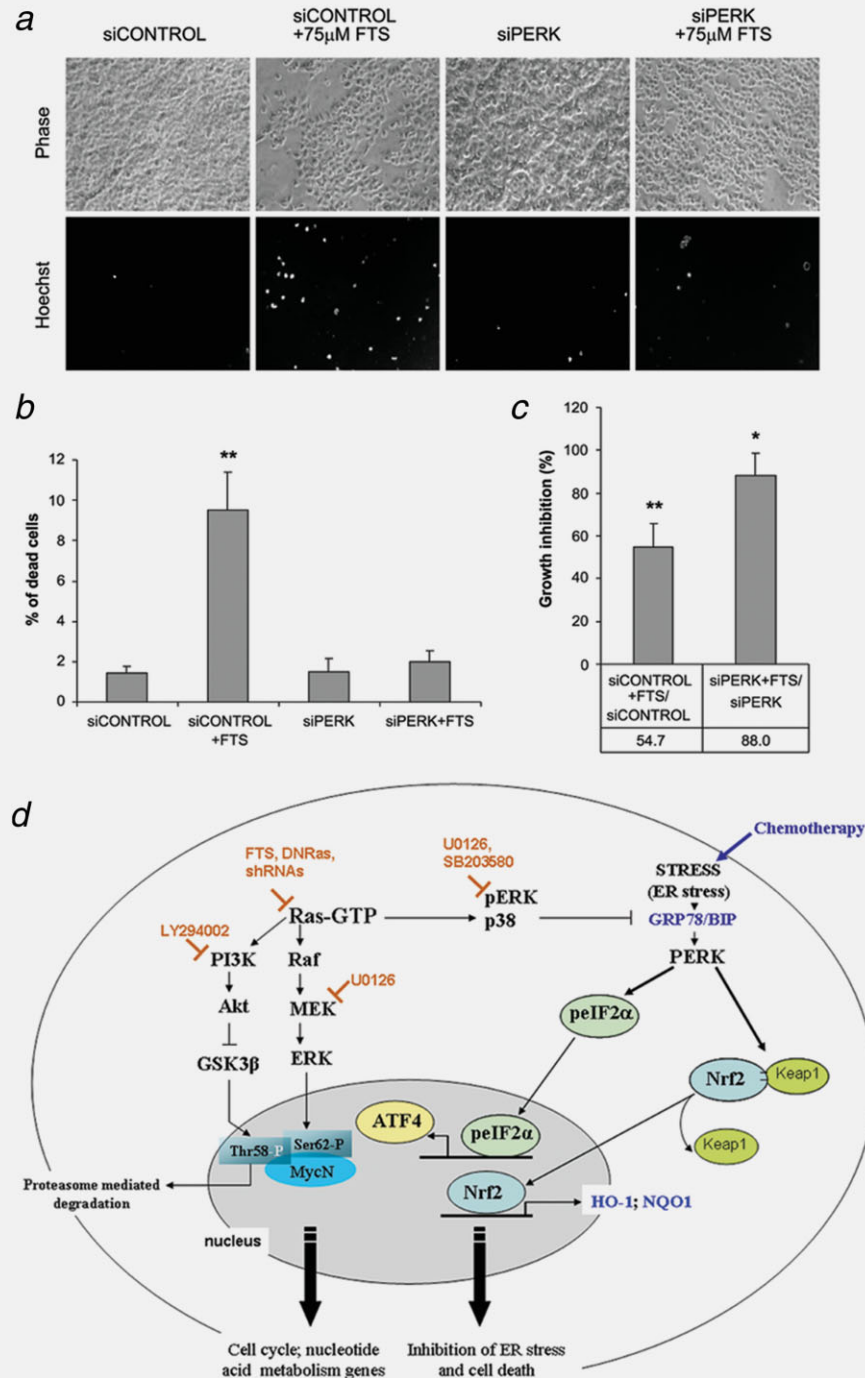


**Figure 6.** siRNA to PERK attenuates stress and prevents death induced in LAN-1 cells by farnesylthiosalicylic acid (FTS). (a–c) LAN-1 cells ( $5 \times 10^5$  cells/well in 6-well plates) were transfected with either PERK siRNA SMARTpool (*siPERK*) or *siCONTROL* (nontargeting pool). Medium was replaced by 5% FCS media 1 day later, and the cells were incubated with 75  $\mu$ M FTS or vehicle control for an additional 24 hr and then stained with Hoechst, as described in Material and Methods. (a) Cells were visualized under a fluorescence microscope ( $\times 20$ ). Typical phase and fluorescence images are shown. Images recorded in 5 distinct fields in each of 2 separate wells were quantified by counting the total number of cells and the number of fluorescently labeled (dead) cells. (b) Numbers of dead cells, calculated as a percentage of the total number of cells (means  $\pm$  SD,  $n = 10$ ). (c) Growth inhibition, expressed as the number of FTS-treated cells in each transfection calculated as a percentage of the number of control cells ( $n = 10$ ,  $*p < 0.05$ ,  $**p < 0.001$ , Student's *t*-test). (d) Model depicting disruption of Ras and Myc cooperation by Ras inhibitors in cancer cells with activated Ras and amplified *Myc* gene, leading to cell-cycle arrest and endoplasmic reticulum (ER) stress. Active Ras-GTP protein stabilizes Myc protein through the Raf/MEK/ERK and PI3K/Akt cascades, preventing its proteasomal degradation and thus facilitating cell-cycle progression and regulation of cellular homeostasis.<sup>29,39</sup> Active Ras, operating through ERK and p38, also negatively regulates BIP, leading to its decrease and hence a decrease in PERK activation.<sup>31</sup> PERK serves as the central regulator of translational control during the UPR. Active PERK activates eIF2 $\alpha$  and Nrf2.<sup>40</sup> Negative regulation of PERK by Ras results in downregulation of eIF2 $\alpha$  and Nrf2 and inhibition of ER stress.<sup>31,40</sup> Persistent ER stress induces a switch in UPR signaling from prosurvival to proapoptotic pathways. The case of cells with amplified *Myc* and active Ras that are treated for prolonged periods with farnesylthiosalicylic acid (FTS) resembles the prosurvival to proapoptotic switch described here. The proposed mechanism is postulated to enhance the FTS-induced killing of cancer cells.

## Discussion

Here, we showed that reduction in the levels of Ras is accompanied by strong downregulation of Myc not only in neuroblastoma cells (7; Fig. 1) but also in myeloma and leukemia cells with amplified *c-Myc* (Figs. 2c and 2d). Thus, active Ras stabilizes MycN and *c-Myc* in cancer cells.<sup>41</sup> Robust changes in gene expression were observed in LAN-1 and 2 other cell lines (NCIH929 and K562) with amplified *Myc*. In addition to the known downregulation of the transcription factors E2F and NF-Y by FTS, which results in cell growth arrest,<sup>17</sup> we detected, in all 3 cell lines, a novel pattern of transcriptional response to FTS, namely upregulation of the transcription factors Nrf2, ATF3 and ATF4, all known to play a role in ER stress induction, as reflected by the UPR.<sup>31</sup> The activity of FTS in simultaneously inhibiting cell-cycle progression and inducing ER stress appears to lead to the death of cancer cells that harbor active Ras and amplified *Myc*. This is consistent with earlier studies showing that induction of cell growth arrest, coupled with the prolonged decrease in protein translation that typically occurs during the UPR, initiates apoptosis.<sup>42</sup> In line with a combined action of FTS on stress-related transcription factors and on *Myc* are the known functions of *Myc* in metabolic pathways, such as amino acid and nucleotide synthesis, which regulate cellular homeostasis in response to oxidative stress.<sup>29</sup>

Our results show that the ER response to stress (the UPR) is negatively regulated by Ras in cells with active Ras and amplified *Myc*. This strongly suggests that active Ras and *Myc* cooperatively block ER stress. We found that FTS or DN-Ras or shRNA to Ras isoforms induce ER stress (Fig. 5). These strengthen the notion that FTS indeed reduced the level of active Ras in the cell membrane. We do not know of other fransylated proteins that are inhibited by FTS reducing *Myc* and increasing ER stress. We also showed that inhibitors of p38 and MEK induce an increase in BIP and Nrf2, and that siRNA to PERK induces a decrease in Nrf2 and ATF4 and rescues the cells from death induced by FTS (Figs. 5 and 6). We therefore conclude that the ER stress cascades BIP/PERK/Nrf2 and eIF2 $\alpha$ /ATF4/ATF3 are negatively regulated by Ras through its effectors ERK and p38 (<sup>43–45</sup>; Fig. 6d). On the basis of early studies and the present results, we propose a model in which the active Ras-GTP stabilizes *Myc* protein through the Raf/MEK/ERK and PI3K/Akt cascades, facilitating cell-cycle progression and regulating cellular homeostasis.<sup>29,39</sup> Our model can also explain how amplified *Myc* exerts its Ras-dependent protection of the cells from ER stress-associated death (Fig. 6d). The mechanisms underlying typical stress responses and control of protein synthesis have been well characterized. The stress kinases GCN2, HRI and PERK are activated by different stress signals.<sup>46,47</sup> Of these kinases, PERK serves as the central regulator of translational control during the UPR.<sup>48</sup> Because active PERK activates eIF2 $\alpha$  and Nrf2,<sup>40</sup> the negative regulation of PERK by Ras results in downregulation of these 2 transcription factors and inhibition of ER stress (<sup>31,40</sup>; Fig. 6d).

Notably, prolonged ER stress is reportedly coupled to cell-cycle arrest, which apparently prevents cell repair and leads to cell death.<sup>48</sup> The persistent ER stress induces a switch in UPR signaling, from prosurvival to proapoptotic pathways, such as the induction of CHOP (a proapoptotic transcription factor) and GADD34 (a cofactor of eIF2 $\alpha$  phosphatase). This switch is activated by the PERK-eIF2 $\alpha$  pathway by activation of proapoptotic kinases such as ASK1, and JNK through the IRE-1 pathway.<sup>31,49,50</sup> Therefore, cells with active Ras and amplified *Myc* exhibit facilitated proliferation and attenuated ER stress and death. Disruption of the cooperation between Ras and *Myc* by inhibitors such as FTS leads to attenuation of cell growth and to increased ER stress, as we showed here. Treatment of such cells for prolonged periods with FTS resembles the prosurvival to proapoptosis switch described earlier and as shown in our experiments (Figs. 1–3). It is interesting to note that ER stress was shown to be driven in primary melanocytes by the oncogenic H-Ras (G12V) but not by oncogenic N-Ras.<sup>51</sup> These data show that both, the Ras isoform and the cellular context, determine the ER response and the UPR leading to cell death.

We postulate that the protective effects of Ras and *Myc* in cancer cells are achieved by regulation of antioxidant proteins to mitigate the detrimental effects of excessive oxidative stress incurred by the tumor cells. This hypothesis is strengthened by the reported observation that H-Ras-transformed tumorigenic T29H cells (ovarian carcinoma) are much more resistant to H<sub>2</sub>O<sub>2</sub>-mediated cell killing than are the immortalized nontumorigenic parental T29 cells. Pretreatment of T29H cells with FTI-277 for 24 hr resulted in a marked decrease in their resistance to H<sub>2</sub>O<sub>2</sub>-induced cell death relative to control DMSO-treated cells.<sup>52</sup> This finding suggests that Ras is a direct participant in the resistance to apoptosis mediated by reactive oxygen species in transformed cells, which might explain the pattern of upregulated genes in LAN-1 cells as a result of reduction in the levels of Ras by FTS (Supporting Information Tables 1 and 2). Moreover, overexpression of HO-1 was found to exert dual effects under oxidative stress and might have effects that are detrimental rather than cytoprotective.<sup>53</sup> Our results show that expression of HO-1 was increased by FTS in all 3 cell lines harboring amplified *Myc* (Fig. 3c), supporting the possible participation of HO-1 in FTS-induced death.

To summarize, we identified a core transcriptional response to the inhibition of Ras in cells with active Ras and amplified *Myc*. This finding suggests that ER stress genes might account for the observed FTS-induced cell growth arrest and the ER stress response, which together lead to cell death under conditions of reduced levels of Ras and increased *Myc* protein degradation. Thus, Ras and *Myc*, acting cooperatively, appear to negatively regulate ER stress, conferring resistance to cell death. Although the expression of stress gene responses elicited by the Ras inhibitor FTS are protective, there are also other effects, which are relatively

stressor-specific and can lead to cell death. Both types of stress mechanisms presented here, namely the BIP/PERK/Nrf2 and the eIF2 $\alpha$ /ATF4/ATF3 cascades (Fig. 6d), have the potential for therapeutic intervention. In this regard, it is important to note that chemotherapeutic drugs are known to induce ER stress (<sup>40</sup>; Fig. 6d). Treatment of human cancer cell lines with a combination of FTS and chemotherapy, even when amplified *Myc* was not known to be present, enhanced the chemotherapeutic effect. In pancreatic cancer cells, for example, FTS synergizes with gemcitabine and enhances its killing effect.<sup>54</sup> Similar findings were observed with doxorubicin and FTS in melanoma cancer cells.<sup>55</sup> This study strongly

suggests that combined treatment with FTS and chemotherapy might be beneficial in cells with chronically active Ras and amplified *Myc*.

### Acknowledgements

This work was supported in part by The Israel Science Foundation (Dr. Y. Kloog) and by the Prais-Drimmer Institute for The Development of Anti-Degenerative Drugs (S.Y.-S. and Y.-K.). Dr. G. Rechavi is the incumbent of the Djerassi Chair in Oncology and Y. Kloog is the incumbent of the Jack H. Skirball Chair in Applied Neurobiology. The authors thank Ms. S.R. Smith for editorial assistance and Dr. R. Elkon for his support and advice on the gene profiling and clustering analysis.

### References

- Bourne HR, Sanders DA, McCormick F. The GTPase superfamily: conserved structure and molecular mechanism. *Nature* 1991;349:117–27.
- Shields JM, Pruitt K, McFall A, Shaub A, Der CJ. Understanding Ras: 'it ain't over 'til it's over'. *Trends Cell Biol* 2000;10:147–54.
- Bos JL. ras oncogenes in human cancer: a review. *Cancer Res* 1989;49:4682–9.
- Basu TN, Gutmann DH, Fletcher JA, Glover TW, Collins FS, Downward J. Aberrant regulation of ras proteins in malignant tumour cells from type 1 neurofibromatosis patients. *Nature* 1992;356:713–15.
- Scheffzek K, Ahmadian MR, Wittinghofer A. GTPase-activating proteins: helping hands to complement an active site. *Trends Biochem Sci* 1998;23:257–62.
- Sears R, Nuckolls F, Haura E, Taya Y, Tamai K, Nevins JR. Multiple Ras-dependent phosphorylation pathways regulate Myc protein stability. *Genes Dev* 2000;14:2501–14.
- Yaari S, Jacob-Hirsch J, Amariglio N, Haklai R, Rechavi G, Kloog Y. Disruption of cooperation between Ras and MycN in human neuroblastoma cells promotes growth arrest. *Clin Cancer Res* 2005;11:4321–30.
- Sears RC, Nevins JR. Signaling networks that link cell proliferation and cell fate. *J Biol Chem* 2002;277:11617–20.
- Bachireddy P, Bendapudi PK, Felsher DW. Getting at MYC through RAS. *Clin Cancer Res* 2005;11:4278–81.
- Wong AJ, Ruppert JM, Eggleston J, Hamilton SR, Baylin SB, Vogelstein B. Gene amplification of c-myc and N-myc in small cell carcinoma of the lung. *Science* 1986;233:461–4.
- Knyazev PG, Fedorov SN, Serova OM, Pluzhnikova GF, Novikov LB, Kalinovsky VP, Seitz JF. Molecular-genetic analysis of myc and c-Ha-ras proto-oncogene alterations in human carcinoma. *Haematol Blood Transfus* 1987;31:469–73.
- Kohl NE, Gee CE, Alt FW. Activated expression of the N-myc gene in human neuroblastomas and related tumors. *Science* 1984;226:1335–7.
- Ernst TJ, Gazdar A, Ritz J, Shipp MA. Identification of a second transforming gene, *rasn*, in a human multiple myeloma line with a rearranged c-myc allele. *Blood* 1988;72:1163–7.
- Sawyers CL, McLaughlin J, Witte ON. Genetic requirement for Ras in the transformation of fibroblasts and hematopoietic cells by the Bcr-Abl oncogene. *J Exp Med* 1995;181:307–13.
- Moley JF, Brother MB, Wells SA, Spengler BA, Biedler JL, Brodeur GM. Low frequency of ras gene mutations in neuroblastomas, pheochromocytomas, and medullary thyroid cancers. *Cancer Res* 1991;51:1596–9.
- Delgado MD, Vaque JP, Arozarena I, Lopez-Illasaca MA, Martinez C, Crespo P, Leon J. H-, K- and N-Ras inhibit myeloid leukemia cell proliferation by a p21WAF1-dependent mechanism. *Oncogene* 2000;19:783–90.
- Blum R, Elkon R, Yaari S, Zundelevich A, Jacob-Hirsch J, Rechavi G, Shamir R, Kloog Y. Gene expression signature of human cancer cell lines treated with the ras inhibitor salirasib (S-farnesylthio-salicylic acid). *Cancer Res* 2007;67:3320–8.
- Elad-Sfadia G, Haklai R, Ballan E, Gabius HJ, Kloog Y. Galectin-1 augments Ras activation and diverts Ras signals to Raf-1 at the expense of phosphoinositide 3-kinase. *J Biol Chem* 2002;277:37169–75.
- Shamir R, Maron-Katz A, Tanay A, Linhart C, Steinfeld I, Sharan R, Shiloh Y, Elkon R. EXPANDER—an integrative program suite for microarray data analysis. *BMC Bioinformatics* 2005;6:232.
- Sharan R, Shamir R. CLICK: a clustering algorithm with applications to gene expression analysis. *Proc Int Conf Intell Syst Mol Biol* 2000;8:307–16.
- Niv H, Gutman O, Henis YI, Kloog Y. Membrane interactions of a constitutively active GFP-K-Ras 4B and their role in signaling: evidence from lateral mobility studies. *J Biol Chem* 1999;274:1606–13.
- Cohen N, Novikov I, Hardan I, Esa A, Brok-Simoni F, Amariglio N, Rechavi G, Ben-Bassat I, Trakhtenbrot L. Standardization criteria for the detection of BCR/ABL fusion in interphase nuclei of chronic myelogenous leukemia patients by fluorescence in situ hybridization. *Cancer Genet Cytogenet* 2000;123:102–8.
- Mor A, Keren G, Kloog Y, George J. N-Ras or K-Ras inhibition increases the number and enhances the function of Foxp3 regulatory T cells. *Eur J Immunol* 2008;38:1493–502.
- Blum R, Jacob-Hirsch J, Amariglio N, Rechavi G, Kloog Y. Ras inhibition in glioblastoma down-regulates hypoxia-inducible factor-1 $\alpha$ , causing glycolysis shutdown and cell death. *Cancer Res* 2005;65:999–1006.
- Elkon R, Linhart C, Sharan R, Shamir R, Shiloh Y. Genome-wide in silico identification of transcriptional regulators controlling the cell cycle in human cells. *Genome Res* 2003;13:773–80.
- Berkovich E, Ginsberg D. Ras induces elevation of E2F-1 mRNA levels. *J Biol Chem* 2001;276:42851–6.
- Gu Z, Kuntz-Simon G, Rommelaere J, Cornelis J. Oncogenic transformation-dependent expression of a transcription factor NF-Y subunit. *Mol Carcinog* 1999;24:294–9.
- Boon K, Caron HN, van Asperen R, Valentijn L, Hermus MC, van Sluis P, Roobeek I, Weis I, Voute PA, Schwab M, Versteeg R. N-myc enhances the expression of a large set of genes functioning in ribosome biogenesis and protein synthesis. *EMBO J* 2001;20:1383–93.
- Dang CV. c-Myc target genes involved in cell growth, apoptosis, and metabolism. *Mol Cell Biol* 1999;19:1–11.

30. Jaiswal AK. Nrf2 signaling in coordinated activation of antioxidant gene expression. *Free Radic Biol Med* 2004;36:1199–207.
31. Cullinan SB, Diehl JA. Coordination of ER and oxidative stress signaling: the PERK/Nrf2 signaling pathway. *Int J Biochem Cell Biol* 2006;38:317–32.
32. Wek RC, Jiang HY, Anthony TG. Coping with stress: eIF2 kinases and translational control. *Biochem Soc Trans* 2006;34:7–11.
33. McCullough KD, Martindale JL, Klotz LO, Aw TY, Holbrook NJ. Gadd153 sensitizes cells to endoplasmic reticulum stress by down-regulating Bcl2 and perturbing the cellular redox state. *Mol Cell Biol* 2001;21:1249–59.
34. Hetz C, Bernasconi P, Fisher J, Lee AH, Bassik MC, Antonsson B, Brandt GS, Iwakoshi NN, Schinzel A, Glimcher LH, Korsmeyer SJ. Proapoptotic BAX and BAK modulate the stress-activated protein response by a direct interaction with IRE1alpha. *Science* 2006;312:572–6.
35. Rotblat B, Ehrlich M, Haklai R, Kloog Y. The Ras inhibitor farnesylthiosalicylic acid (Salirasib) disrupts the spatiotemporal localization of active Ras: a potential treatment for cancer. *Methods Enzymol* 2008;439:467–89.
36. Kietzmann T, Samoylenko A, Immenschuh S. Transcriptional regulation of heme oxygenase-1 gene expression by MAP kinases of the JNK and p38 pathways in primary cultures of rat hepatocytes. *J Biol Chem* 2003;278:17927–36.
37. Bogoyevitch MA, Gillespie-Brown J, Ketterman AJ, Fuller SJ, Ben-Levy R, Ashworth A, Marshall CJ, Sugden PH. Stimulation of the stress-activated mitogen-activated protein kinase subfamilies in perfused heart. p38/RK mitogen-activated protein kinases and c-Jun N-terminal kinases are activated by ischemia/reperfusion. *Circ Res* 1996;79:162–73.
38. Dent P, Yacoub A, Contessa J, Caron R, Amorino G, Valerie K, Hagan MP, Grant S, Schmidt-Ullrich R. Stress and radiation-induced activation of multiple intracellular signaling pathways. *Radiat Res* 2003;159:283–300.
39. Chang F, Lee JT, Navolanic PM, Steelman LS, Shelton JG, Blalock WL, Franklin RA, McCubrey JA. Involvement of PI3K/Akt pathway in cell cycle progression, apoptosis, and neoplastic transformation: a target for cancer chemotherapy. *Leukemia* 2003;17:590–603.
40. Cullinan SB, Zhang D, Hannink M, Arvaisis E, Kaufman RJ, Diehl JA. Nrf2 is a direct PERK substrate and effector of PERK-dependent cell survival. *Mol Cell Biol* 2003;23:7198–209.
41. Sears R, Leone G, DeGregori J, Nevins JR. Ras enhances Myc protein stability. *Mol Cell* 1999;3:169–79.
42. Keum YS, Jeong WS, Kong AN. Chemoprevention by isothiocyanates and their underlying molecular signaling mechanisms. *Mutat Res* 2004;555:191–202.
43. Downward J. Targeting RAS signalling pathways in cancer therapy. *Nat Rev Cancer* 2003;3:11–22.
44. Mitin N, Rossman KL, Der CJ. Signaling interplay in Ras superfamily function. *Curr Biol* 2005;15:R563–R574.
45. Smalley KS, Eisen TG. Farnesyl thiosalicylic acid inhibits the growth of melanoma cells through a combination of cytostatic and pro-apoptotic effects. *Int J Cancer* 2002;98:514–22.
46. Berlanga JJ, Santoyo J, De Haro C. Characterization of a mammalian homolog of the GCN2 eukaryotic initiation factor 2alpha kinase. *Eur J Biochem* 1999;265:754–62.
47. Clemens MJ, Elia A. The double-stranded RNA-dependent protein kinase PKR: structure and function. *J Interferon Cytokine Res* 1997;17:503–24.
48. Harding HP, Zhang Y, Bertolotti A, Zeng H, Ron D. Perk is essential for translational regulation and cell survival during the unfolded protein response. *Mol Cell* 2000;5:897–904.
49. Oyadomari S, Mori M. Roles of CHOP/GADD153 in endoplasmic reticulum stress. *Cell Death Differ* 2004;11:381–9.
50. Roux PP, Blenis J. ERK and p38 MAPK-activated protein kinases: a family of protein kinases with diverse biological functions. *Microbiol Mol Biol Rev* 2004;68:320–44.
51. Denoyelle C, Abou-Rjaily G, Bezrookove V, Verhaegen M, Johnson TM, Fullen DR, Pointer JN, Gruber SB, Su LD, Nikiforov MA, Kaufman RJ, Bastian BC, et al. Anti-oncogenic role of the endoplasmic reticulum differentially activated by mutations in the MAPK pathway. *Nat Cell Biol* 2006;8:1053–63.
52. Young TW, Mei FC, Yang G, Thompson-Lanza JA, Liu J, Cheng X. Activation of antioxidant pathways in ras-mediated oncogenic transformation of human surface ovarian epithelial cells revealed by functional proteomics and mass spectrometry. *Cancer Res* 2004;64:4577–84.
53. Hsieh CH, Rau CS, Hsieh MW, Chen YC, Jeng SF, Lu TH, Chen SS. Simvastatin-induced heme oxygenase-1 increases apoptosis of Neuro 2A cells in response to glucose deprivation. *Toxicol Sci* 2008;101:112–21.
54. Gana-Weisz M, Halaschek-Wiener J, Jansen B, Elad G, Haklai R, Kloog Y. The Ras inhibitor S-trans,trans-farnesylthiosalicylic acid chemosensitizes human tumor cells without causing resistance. *Clin Cancer Res* 2002;8:555–65.
55. Halaschek-Wiener J, Kloog Y, Wacheck V, Jansen B. Farnesyl thiosalicylic acid chemosensitizes human melanoma in vivo. *J Invest Dermatol* 2003;120:109–15.